Author(s): McCrea-Hendrick, Madison L.; Caputo, Christine A.; Linnera, Jarno; Vasko, Petra; Weinstein, Cory M.; Fettinger, James C.; Tuononen, Heikki; Power, Philip P.

Title: Cleavage of Ge–Ge and Sn–Sn Triple Bonds in Heavy Group 14 Element Alkyne Analogues (EAriPr4)2 (E = Ge, Sn; AriPr4 = C6H3-2,6(C6H3-2,6-iPr2)2) by Reaction with Group 6 Carbonyls

Year: 2016

Version:

Please cite the original version:

McCrea-Hendrick, M. L., Caputo, C. A., Linnera, J., Vasko, P., Weinstein, C. M., Fettinger, J. C., Tuononen, H., & Power, P. P. (2016). Cleavage of Ge–Ge and Sn–Sn Triple Bonds in Heavy Group 14 Element Alkyne Analogues (EAriPr4)2 (E = Ge, Sn; AriPr4 = C6H3-2,6(C6H3-2,6-iPr2)2) by Reaction with Group 6 Carbonyls. Organometallics, 35(16), 2759-2767. https://doi.org/10.1021/acs.organomet.6b00519

Cleavage of Ge-Ge and Sn-Sn Triple Bonds in Heavy Group 14 Element Alkyne Analogues (EAr^{iPr4})$_2$ (E = Ge, Sn; Ar^{iPr4} = C_6H_3-2,6(C_6H_3-2,6-$^iPr_2$)$_2$) by Reaction with Group 6 Carbonyls

Madison L. McCrea-Hendrick,[†] Christine A. Caputo,[1,†] Jarno Linnera,[‡] Petra Vasko,[‡] Cory M. Weinstein,[2,†] James C. Fettinger,[†] Heikki M. Tuononen,[‡,] and Philip P. Power[†,*]*

[†] Department of Chemistry, 1 Shields Avenue, University of California Davis, Davis, CA, USA 95616. Fax: +1-530-732-8995; Tel: +1-530-752-8900; E-mail: pppower@ucdavis.edu

[‡] Department of Chemistry, Nanoscience Center, University of Jyväskylä, P.O. Box 35, FI-40014 University of Jyväskylä, Finland. Tel: +358-40-805-3713; E-mail: heikki.m.tuononen@jyu.fi

[1] Present Address: Department of Chemistry, University of New Hampshire, Durham, NH, USA 03824.
[2] Present Address: Department of Chemistry and Biochemistry, University of California San Diego, La Jolla, CA, USA 92093.

ABSTRACT

The reactions of heavier group 14 element alkyne analogues (EAr^{iPr4})$_2$ (E = Ge, Sn; Ar^{iPr4} = C_6H_3-2,6-(C_6H_3-2,6-$^iPr_2$)$_2$) with the group 6 transition metal carbonyls $M(CO)_6$ (M = Cr, Mo, W) under UV irradiation resulted in the cleavage of the E-E bond and the formation of complexes {$Ar^{iPr4}EM(CO)_4$}$_2$ (**1**–**6**) that were characterized by single crystal X-ray diffraction as well as by IR and multinuclear NMR spectroscopies. Single crystal X-ray structural analyses of **1**–**6** showed that the complexes have a nearly planar rhomboid M_2E_2 core with three-coordinate group 14 atoms. The coordination geometry at the group 6 metals is distorted octahedral formed by four carbonyl groups as well as two bridging EAr^{iPr4} units. IR spectroscopic data suggest that the EAr^{iPr4} units are not very efficient π-acceptors, but the investigation of E-M metal-metal interactions in **1**–**6** with computational methods revealed the importance of both σ- and π-type contributions to bonding. The mechanism for the insertion of transition metal carbonyls into E-E bonds in (EAr^{iPr4})$_2$ was also probed computationally.

INTRODUCTION

The heavier group 14 element analogues of acetylene, the dimetallynes $(ER)_2$ (E = Si, Ge, Sn, Pb), were reported as stable species in the first decade of the new millennium.[1] Their bonding and structures differ considerably from that in analogous carbon congeners in that all dimetallynes feature *trans*-bent geometries in which the degree of bending increases with the atomic number of the group 14 element.

The bonding in dimetallynes can be represented by the valence bond structures shown in Scheme 1.[2] An alternative view of bonding in dimetallynes is provided by molecular orbital (MO) theory. An illustration of the effects of bending on the frontier molecular orbitals provides a useful basis upon which the reactions undergone by dimetallynes can be rationalized (Scheme 2).

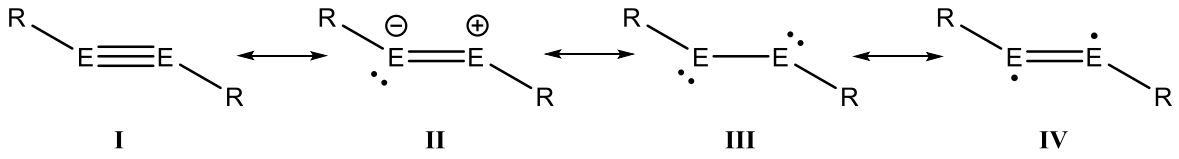

Scheme 1. Resonance structures for heavier group 14 alkyne analogues (E = Si, Ge, Sn, Pb; R = organic ligand).

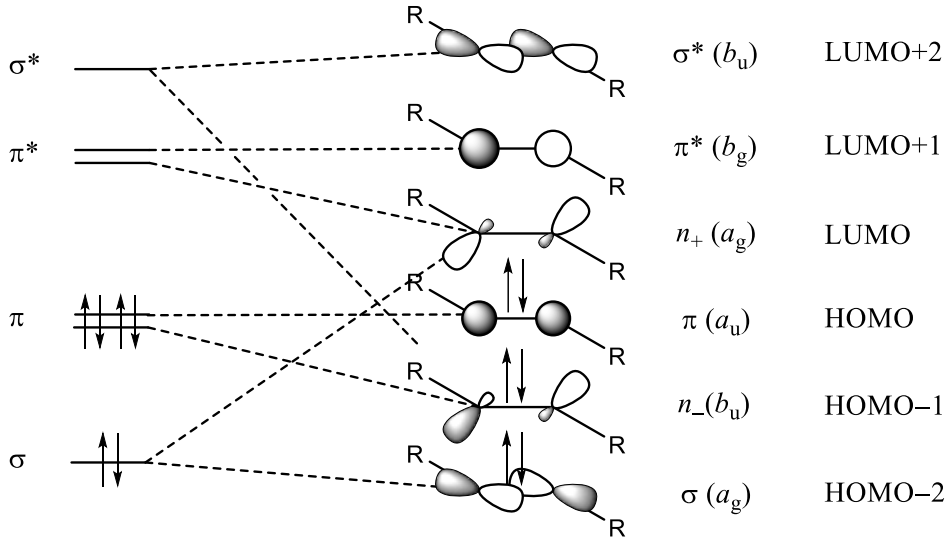

Scheme 2. Schematic depiction of frontier molecular orbitals in heavier group 14 alkyne analogues REER (E = Si, Ge, Sn, Pb; R = organic ligand). The exact ordering of frontier orbitals depends on the element E and the substituent R.

In effect, in the local C_{2h} point group symmetry of the bent geometry, the in plane π-orbital and the σ^*-orbital have the same symmetry properties and can mix to afford the slipped π-type HOMO−1 orbital of dimetallynes that is primarily non-bonding in character (n_-, b_u symmetry), provided that the energies of the orbitals differ by less than *ca.* 4 eV from each other.[2] Thus, the bending of the molecular framework results in lifting of the degeneracy of the original π-level in the linear structure and the out of plane π-orbital (a_u symmetry) becomes the HOMO of dimetallynes. The degeneracy of the original π^*-level is lifted in a similar fashion, for which reason the LUMO of dimetallynes is non-bonding in character (n_+, a_g symmetry). It should be noted, however, that the exact ordering of frontier orbitals of REER depends on the element E and, to some extent, on the substituent R.

The results from extensive studies of the physical and chemical properties of dimetallynes are consistent with the above bonding picture.[2] For example, dimetallynes can be readily reduced by the addition of one or two electrons to their low-lying non-bonding LUMO by simple treatment with alkali metals in solution.[3] The low-lying LUMO of dimetallynes is also consistent with coordination of Lewis bases such as *tert*-butyl isonitrile or an *N*-heterocyclic carbene (NHC) in the molecular plane rather than perpendicular to it, which is what would be expected if the LUMO remained a π^*-type orbital.[4] Furthermore, the frontier orbitals of dimetallynes are consistent with their high reactivity toward small molecules such as H_2[5,6] as well as amines and boranes.[7] Because of the changes in the frontier orbitals that occur upon bending, the dimetallynes may react rapidly with olefins and alkynes through mechanisms that differ from those of the Woodward-Hoffman rules and are uncharacteristic of carbon-based compounds.[8]

Despite the large number of investigations of the chemistry and properties of dimetallynes, there are relatively few reports of dimetallynes acting as electron donors in a transition metal complex. The first reported example was $[Ag(GeAr^{iPr4})_2][SbF_6]$ in which the neutral digermyne binds to a Ag^+ ion in η^2-fashion.[9] Similar complexes of a related dialkyldisilyne complex of palladium and platinum have been realized by Iwamoto and coworkers.[10] In addition, Sekiguchi, Driess and coworkers have reported the reaction of a disilyne $\{SiSi^iPr[CH(SiMe_3)_2]_2\}_2$ with an NHC to give a coordination complex in which the electronic structure of the disilyne corresponds

to the resonance structure **II** in Scheme 1 (Scheme 3).[4b] Subsequent reaction of the NHC-disilyne complex with $ZnCl_2$ afforded an NHC-disilyne-$ZnCl_2$ complex in which the disilyne has *cis* geometry rather than *trans* and behaves simultaneously as a donor and an acceptor in push-pull fashion. A similar donor-acceptor complex has also been obtained via reaction of the disilyne $\{SiSi^iPr[CH(SiMe_3)_2]_2\}_2$ with methyllithium.[11]

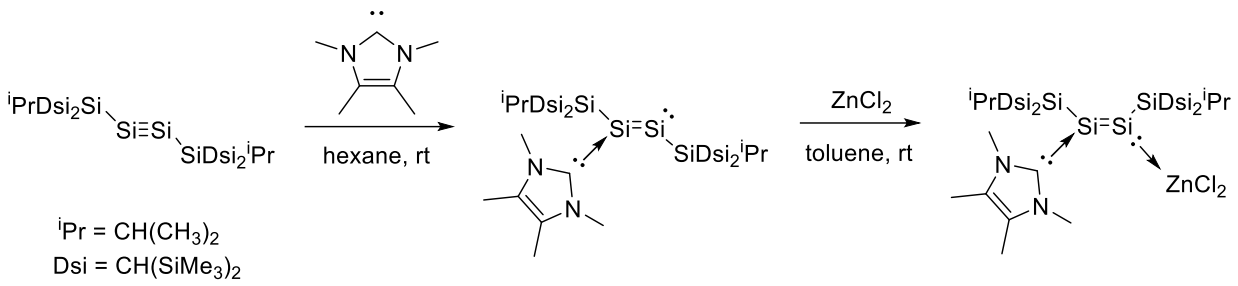

Scheme 3. Synthesis of Sekiguchi's and Driess' "push-pull" NHC-disilyne-$ZnCl_2$ complex.[4b]

In order to explore the complexing properties of group 14 dimetallynes $(EAr^{iPr4})_2$ (E = Ge, Sn) further, we have now investigated their reactivity with group 6 transition metal carbonyls $M(CO)_6$ (M = Cr, Mo, W) under photoirradiation (Scheme 4). In this instance, the isolated products were not simple Lewis acid-base adducts but dinuclear metal complexes with the general formula $\{Ar^{iPr4}EM(CO)_4\}_2$ that result from cleavage of the formal E-E triple bond with successive complexation of two $M(CO)_4$ fragments that bridge the EAr^{iPr4} units.

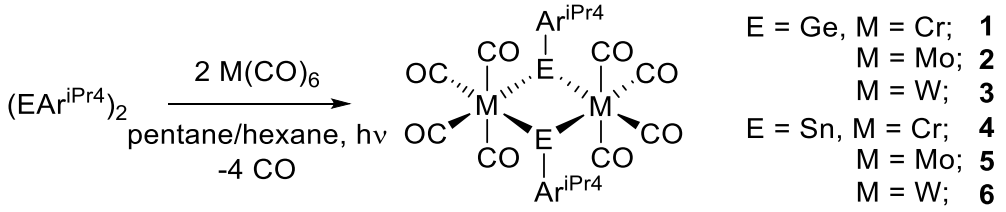

Scheme 4. Synthesis of complexes $\{Ar^{iPr4}EM(CO)_4\}_2$ (**1**–**6**; E = Ge, Sn; M = Cr, Mo, W).

RESULTS AND DISCUSSION

Synthesis. Complexes **1**–**6** were synthesized by combining one equivalent of $(EAr^{iPr4})_2$ (E = Ge, Sn) with two equivalents of $M(CO)_6$ (M = Cr, Mo, W) in either hexane or pentane in a quartz Schlenk flask, followed by irradiation with ultraviolet light for 24 h, during which time the color of the solution changed from dark green (Sn) or bright orange (Ge) to dark red (Sn) or dark

brown (Ge). Upon cooling the solution to room temperature, crystals suitable for X-ray diffraction formed on the sides of the flask. Decanting and concentrating the solution followed by storage in a *ca.* −18°C freezer afforded additional crystals; in case of compound **4**, a saturated solution in toluene was used to grow crystals that were suitable for X-ray diffraction. The products **1**–**6** were isolated in modest yield as dichroic green/red (**1** and **4**), turquoise (**2** and **3**) or brown red (**5** and **6**) crystals.

NMR Spectroscopy. The solution ^{1}H NMR spectra of **1**–**6** displayed signals corresponding to the Ar^{iPr4} ligand with diastereotopic isopropyl methyl groups and a single distinctive methine septet signal that is significantly shielded, possibly as a result of the proximity of the proton to the carbonyl groups perpendicular to the M_2E_2 plane (see below for discussion of structural data). Overall, the ^{1}H NMR chemical shifts of compounds **1**–**6** show very little variation with respect to the group 6 and 14 elements. The corresponding $^{13}C\{^{1}H\}$ NMR spectra revealed two distinct chemical shifts for the carbonyl resonances, which is consistent with the structural data for **1**–**6** (see below). The carbonyl $^{13}C\{^{1}H\}$ NMR resonances shift upfield as the atomic number of the group 6 metal increases.

The $^{119}Sn\{^{1}H\}$ NMR spectra for complexes **4**–**6** were recorded in C_6D_6 solution and referenced externally to $Sn^{n}Bu_4$ in $CDCl_3$. The ^{119}Sn resonances appeared well downfield at 2172.0 (**4**), 2245.9 (**5**) and 2128.8 ppm (**6**). The observed chemical shifts are further downfield than those reported for three-coordinate tin in a range of related transition metal complexes (673–1231 ppm)[12] but are in the same range as that found for group 6 metallo-stannylenes (η^5-C_5H_5)$(CO)_3$MSn-C_6H_3-2,6-Ar_2 (Ar = C_6H_2-2,4,6-Me_3 or C_6H_2-2,4,6-$^{i}Pr_3$) that feature two-coordinate tin atoms (2116–2650 ppm).[13] Thus, complexes **4**–**6** have ^{119}Sn chemical shifts that are more typical of two-coordinate than three-coordinate tin. One notable exception to the above generalization is Fillipou's triple bonded species $Cl(PMe_3)_4$WSn-C_6H_3-2,6-Mes_2 (Mes = C_6H_2-2,4,6-Me_3) that displays a ^{119}Sn resonance at 340 ppm despite having a two-coordinate tin atom.[14]

FT-IR Spectroscopy. Compounds **1**–**3** each show three $\nu_{(CO)}$ stretching bands in their FT-IR spectra. The highest frequency band for each compound occurs at *ca.* 2015 cm^{-1}, while the two other $\nu_{(CO)}$ resonances occur at *ca.* 1980 and 1940 cm^{-1}. Complexes **4**–**6** display four bands, with

the highest $\nu_{(CO)}$ signal at *ca.* 2000 cm^{-1} and the remaining three $\nu_{(CO)}$ stretches at *ca.* 1950, 1935 and 1910 cm^{-1}. Since the structure of the $\{EM(CO)_4\}_2$ moiety in complexes **1**–**6** is close to D_{2h} symmetry (for further structural data, see below), four distinct CO stretching bands are expected. Thus, the three $\nu_{(CO)}$ resonances in complexes **1**–**3** most likely result from coincidental degeneracy of two separate bands. A similar effect has been seen in the group 6 phosphine complexes of Özkar and coworkers.[15]

The $\nu_{(CO)}$ stretching frequencies of **1**–**6** are higher than those in the aryl phosphines of Özkar, which suggests that the bridging EAr^{iPr4} units are better π-acceptors than aryl phosphines. The $\nu_{(CO)}$ stretching frequencies of **1**–**6** can also be compared to those of ethylenediamine (en) complexes with the formula $M(en)(CO)_4$ (M = Cr, Mo, W) reported by Kraihanzel and Cotton.[16] Contrary to the $SnAr^{iPr4}$ and $GeAr^{iPr4}$ units that can act as potential π-acceptors, ethylenediamine has no acceptor orbitals of suitable energy to interact with the $M(CO)_4$ fragment. Thus, the stretching frequencies of Kraihanzel's and Cotton's complexes are lower than in complexes **1**–**6**. In contrast, the group 16 triphenyl phosphite complexes with the formula $M(CO)_4\{P(OC_6H_5)_3\}_2$, reported by Wotiz and coworkers,[17] display $\nu_{(CO)}$ bands that are higher than in **1**–**6** due to the π-acceptor properties of $P(OR)_3$ ligands. However, a computational analysis showed that π-type back-bonding interactions do contribute to M-E bonding in the rhomboid M_2E_2 core of **1**–**6** (see below)

X-Ray Crystallography. Single crystal X-ray diffraction was used to unambiguously determine the structures of compounds **1**–**6** in the solid state. The compounds crystallized in monoclinic space groups $P2_1/n$ (**1** and **4** · **2C$_7$H$_8$**), $C2/c$ (**2** and **3**) and $P2_1/c$ (**5** and **6**), and were found to be essentially isostructural. Selected bond distances and angles for **1**–**6** are listed in Table 1, whereas representative X-ray structure illustrations of complexes **1** and **4** are shown in Figure 1 and 2, respectively.

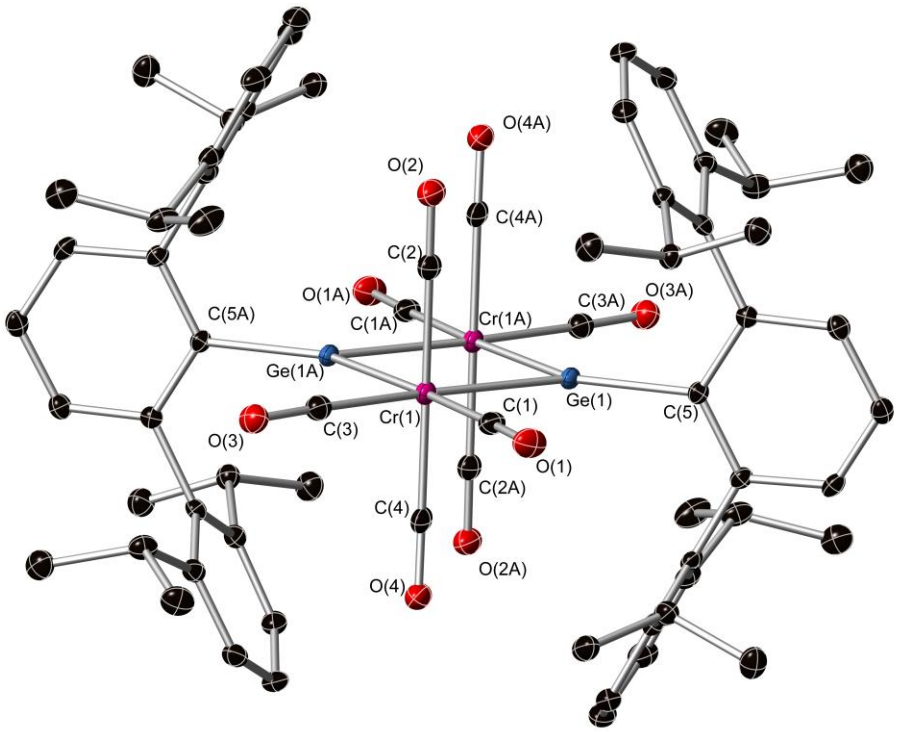

Figure 1. Thermal ellipsoid (30 %) plot of $\{Ar^{iPr4}GeCr(CO)_4\}_2$, **1**. Hydrogen atoms are not shown. Selected bond lengths (Å) and angles (°): Ge(1)-Cr(1) 2.3727(6); Ge(1)-Cr(1A) 2.3821(5); Ge(1)-C(5) 1.951(3); Cr(1)-C(1) 1.865(3); Cr(1)-C(2) 1.915(3); Cr(1)-C(3) 1.866(3); Cr(1)-C(4) 1.917(3); C(1)-O(1) 1.149(4); C(2)-O(2) 1.138(4); C(3)-O(3) 1.148(4); C(4)-O(4) 1.136(4); Cr(1)-Ge(1)-Cr(1A) 79.836(19); C(5)-Ge(1)-Cr(1) 138.75(7); C(5)-Ge(1)-Cr(1A) 141.40(7); Ge(1)-Cr(1)-Ge(1A) 100.164(19); C(2)-Cr(1)-C(4) 178.70(14); C(1)-Cr(1)-C(3) 89.13(14); Ge(1A)-Cr(1)-C(1) 85.08(10); Ge(1)-Cr(1)-C (3) 85.63(9).

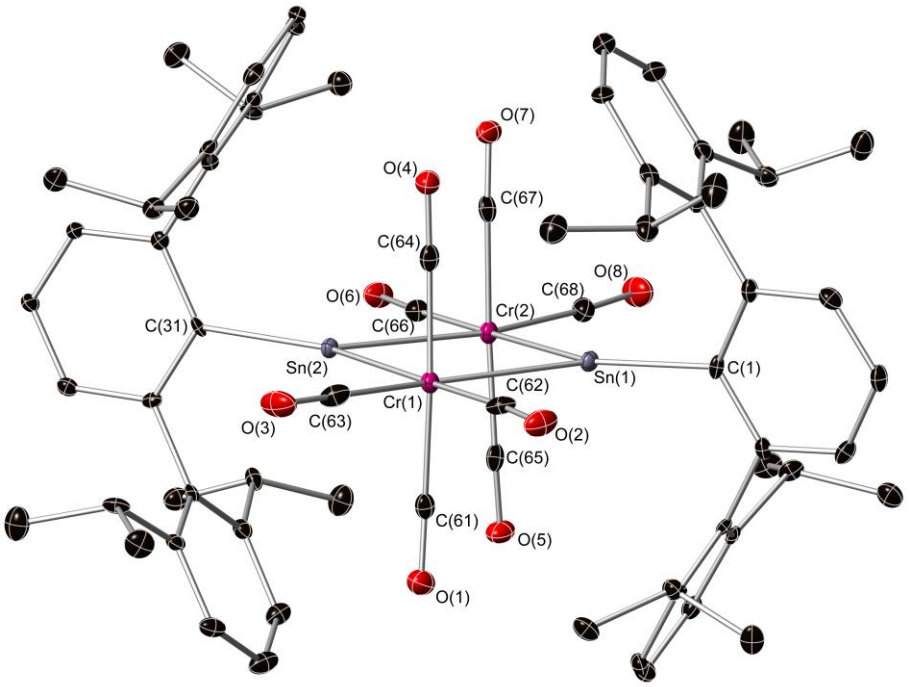

Figure 2. Thermal ellipsoid (30 %) plot of $\{Ar^{iPr4}SnCr(CO)_4\}_2$, **4**. Hydrogen atoms and co-crystallized solvent molecules (toluene) are not shown. Selected bond lengths (Å) and angles (°): Sn(1)-Cr(1) 2.6019(8); Sn(2)-Cr(2) 2.5268(9); Sn(1)-C(1) 2.146(5); Sn(2)-C(31) 2.153(5); Cr(1)-C(61) 1.900(6); Cr(1)-C(62) 1.853(6); Cr(1)-C(63) 1.850(6); Cr(1)-C(64) 1.908(6); Cr(2)-C(65) 1.897(6); Cr(2)-C(66) 1.844(6); Cr(2)-C(67) 1.908(6); Cr(2)-C(68) 1.844(6); C(61)-O(1) 1.155(7); C(62)-O(2) 1.158(7); C(63)-O(3) 1.162(7); C(64)-O(4) 1.147(7); C(65)-O(5) 1.153(7); C(66)-O(6) 1.171(7); C(67)-O(7) 1.151(7); C(68)-O(8) 1.161(8); Cr(1)-Sn(1)-Cr(2) 77.29(3); Cr(1)-Sn(2)-Cr(2) 77.06(3); Sn(1)-Cr(1)-Sn(2) 102.43(3); Sn(1)-Cr(2)-Sn(2) 103.16(3); C(1)-Sn(1)-Cr(1) 132.35(12); C(1)-Sn(1)-Cr(2) 150.21(12); C(31)-Sn(2)-Cr(1) 153.66(12); C(31)-Sn(2)-Cr(2) 129.11(12).

Compounds **1**–**6** have a dimeric $\{Ar^{iPr4}EM(CO)_4\}_2$ (E = Ge, Sn; M = Cr, Mo, W) structure in which the two $M(CO)_4$ fragments bridge the EAr^{iPr4} units. Thus, photoirradiation of group 14 dimetallynes in the presence of group 6 hexacarbonyls has resulted in complete cleavage of the Ge-Ge and Sn-Sn bonds. The cleavage of the formal E-E triple bond in dimetallynes is not entirely unprecedented and is known to take place, for example, in the reaction of $(EAr^{iPr4})_2$ (E = Ge, Sn) with cyclooctatetraene to give an inverse sandwich complex.[18] Similar reactivity has also

been observed for a related amido-digermyne by Jones' and coworkers.[8h] The cleavage of E-E triple bond in dimetallynes has also been observed in the reaction of Sekiguchi's and Driess' disilyne $\{SiSi^{i}Pr[CH(SiMe_3)_2]_2\}_2$ with nitriles,[19] or by the reaction of *m*-terphenyl stabilized digermynes and distannynes with R_2NO or N_2O.[20] However, the insertion of transition metals into E-E bonds in $(EAr^{iPr4})_2$ is a previously unknown transformation.

Table 1. Selected bond lengths [Å] and angles [°] in **1**–**6**.

Compound	E(1)-M(1)	E(1)-M(1A)	E-C_{ipso}	E···E	M···M
1	2.3727(6)	2.3821(5)	1.951(3)	3.6467(7)	3.0511(9)
2	2.5289(9)	2.5042(8)	1.947(5)	3.9001(13)	3.1815(11)
3	2.5404(6)	2.5078(6)	1.941(4)	3.9196(11)	3.1815(5)
4	2.6019(8)	2.5268(9)	2.147(5)	4.0139(7)	3.2034(10)
5	2.6793(4)	2.7429(5)	2.143(2)	4.2982(5)	3.3062(8)
6	2.7514(4)	2.6861(4)	2.138(4)	4.3261(6)	3.2947(5)
Compound	**M(1)-E(1)-M(1A)**	**E(1)-M(1)-E(1A)**	**M(1)-E-C_{ipso}**	**M(1A)-E-C_{ipso}**	**E(1)-M(1)-E(1A)-M(1A)**
1	79.836(19)	100.164(19)	138.75(7)	141.40(7)	0.00(3)
2	78.41(3)	101.59(3)	133.74(19)	147.82(19)	0.00(5)
3	78.130(17)	101.870(17)	133.49(14)	148.34(14)	-0.00(3)
4	77.29(3)	103.16(3)	132.35(12)	150.21(12)	2.05(3)
5	75.131(15)	104.869(15)	130.00(7)	154.86(7)	0.000(18)
6	74.581(10)	105.419(10)	128.97(17)	156.44(17)	-0.00(5)

A central feature in the geometries of complexes **1**–**6** is their planar rhomboid M_2E_2 core. The group 6 metals display octahedral coordination by four carbonyl ligands and two EAr^{iPr4} units, while the coordination of the group 14 metals is trigonal planar. The E···E distances in **1**–**6** are more than 1 Å longer than the sum of Pyykkö-Atsumi single bond covalent radii for two Ge or Sn atoms, 2.42 and 2.80 Å, respectively,[21] suggesting the absence of a covalent bonding interaction. In a similar fashion, the M···M separation between the two $M(CO)_4$ fragments in **1**–**6** exceeds the expected single bond lengths for Cr-Cr, Mo-Mo and W-W bonds (2.40, 2.76 and 2.76 Å, respectively) by more than 0.5 Å. The structures of **1**–**6** are unique in that there are no published reports of metal complexes structurally similar to them with three-coordinate group 14 atoms.

The average Ge-M bond length in complexes **1**–**3** increases from *ca.* 2.38 to 2.52 Å as the group 6 is descended. The Ge-M bonds are only marginally shorter than the sum of Pyykkö-Atsumi single bond covalent radii for the respective elements.[21] It is difficult to draw any

conclusions of the nature of Ge-M interactions in **1**–**3** based on bond length data alone as the bonding between the group 14 element and the transition metal is in general subject to several different influences such as coordination number, oxidation state and orbital type.

The Ge-Cr bond lengths in **1** resemble those previously reported for the germylene complexes $(CO)_5CrGe\{CH(SiMe_3)_2\}_2$ and $(CO)_5CrGe(SMes)_2$ (2.378(4) and 2.367(2) Å, respectively).[22,23] In these two complexes, the germanium atoms are three-coordinate as in **1** but they bind to the chromium atom through their lone pair orbital which has high s-character and therefore a smaller effective radius.[24] In contrast, the Ge-Cr bond in $(\eta^5\text{-}C_5H_5)(CO)_3CrGeAr^{iPr4}$ involves a *p*-type orbital at germanium with a considerably higher effective radius and therefore a significantly longer bond length (2.590(6) Å).[25] The Ge-Mo distances in **2** are similar to those reported by Heinicke and coworkers for the tris-germylene complex *fac*-$(C_2H_2[N(CH_2{}^tBu)]_2Ge)_3Mo(CO)_3$ (2.5325(8), 2.5339(10) and 2.5444(9) Å).[26] Complexes with longer single Ge-Mo bonds have been reported by Jones and coworkers, $Ar^{Ph4}N(C_6H_5)GeMo(\eta^5\text{-}C_5H_5)(CO)_3$ (2.7100(4) Å),[27] as well as by Wang and coworkers, $(\eta^5\text{-}C_5H_3)C(CH_2)_5Mo(CO)_3(Me_2Ge)Mo(CO)_3(\eta^6\text{-}C_5H_3)$ (2.6671(10) Å).[28] The Ge-W bond lengths in **3** can be compared to those in a related germylene complex $(Mes^*Se)_2GeW(CO)_5$ ($Mes^* = C_6H_2\text{-}2,4,6\text{-}{}^tBu_3$) in which germanium is three-coordinate (2.528(1) Å).[29] The complex $IPr(Cl)_2GeW(CO)_5$ (IPr = 1,3-diisopropylimidazolin-2-ylidene), synthesized by Rivard and coworkers, features a four-coordinate Ge atom and has therefore a significantly longer Ge-W bond (2.6351(5) Å) than in **3**.[30]

The trend in Sn-M bonds in **4**–**6** parallels that of the Ge-M bonds in **1**–**3**. The Sn-Cr bonds in **4** are similar to those in the stannylene complex $(CO)_5CrSn\{CH(SiMe_3)_2\}_2$ with three-coordinate tin (2.562(5) Å)[31] and significantly shorter than those in $Cr(SnPh_3)(MeCN)\{P(OMe)_3(CO)_2(NO)\}$ (2.749(1) Å) with a four-coordinate tin atom.[32] Huttner and coworkers have reported a series of group 6 carbonyl complexes featuring Sn-M single bonds stabilized by pyridyl, bipyridyl and phenanthroline ligands.[33] The Sn-Mo and Sn-W bonds in these compounds span a narrow range from 2.744(1) to 2.779(2) Å, and are comparable to the Sn-M bonds in **5** and **6**. In contrast, the Sn-Mo and Sn-W bonds in complexes $Ar^{iPr6}SnM(\eta^5\text{-}C_5H_5)(CO)_3$ involve a *p*-type orbital at tin and have bond lengths that are significantly longer (2.8960(9) and 2.9030(8) Å, respectively) than those in **5** and **6**.[13]

Computational Analyses. The bonding in **1**–**6** is most conveniently described with a fragment based approach. In the following discussion, the complex $\{Ar^{iPr4}GeCr(CO)_4\}_2$ is used as an example case. The complex can be thought of consisting of two fragments: one comprised of the two $Cr(CO)_4$ moieties and the other one comprised of the two bridging $GeAr^{iPr4}$ units. This allows the use of full molecular point group (D_{2h}) throughout the analysis.

Figure 3 shows the frontier orbitals of $\{Ar^{iPr4}GeCr(CO)_4\}_2$ relevant to metal-metal bonding within the Cr_2Ge_2 core along with pertinent fragment orbitals and their contribution to the frontier orbitals of the complex. For simplicity, hydrogen atoms have been used in place of Ar^{iPr4} groups as the identity of the ligand makes only a minor contribution to bonding within the planar rhomboid Cr_2Ge_2 core and can therefore be ignored at the qualitative level.

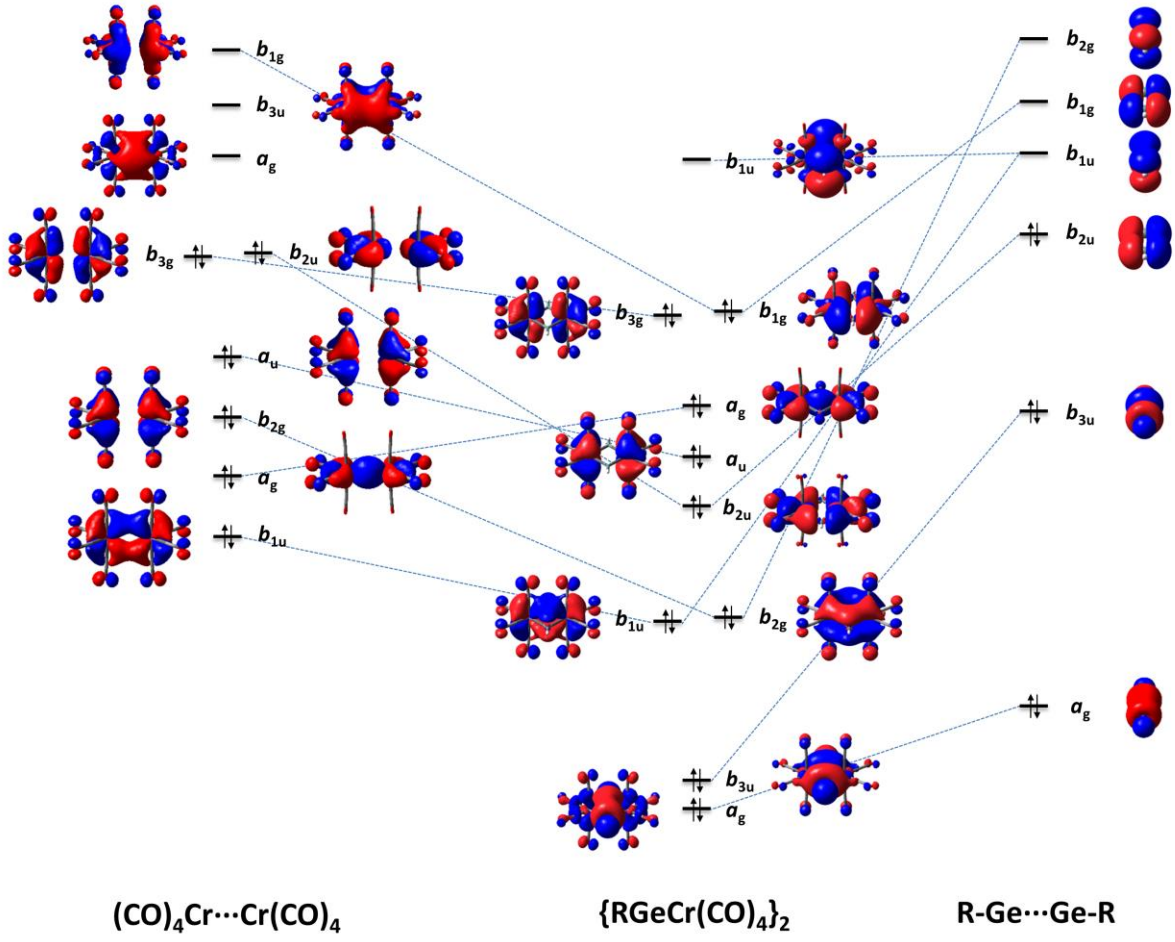

Figure 3. Qualitative orbital diagram illustrating the fragment based description of bonding in the model complex $\{RGeCr(CO)_4\}_2$ (R = H). Orbital energy levels are not drawn to scale.

The b_{1g} symmetric HOMO of $\{HGeCr(CO)_4\}_2$ is a bonding combination of fragment orbitals on both HGe···GeH and $(CO)_4Cr\cdots Cr(CO)_4$, whereas the b_{1u} symmetric LUMO of $\{HGeCr(CO)_4\}_2$ contains a much smaller contribution from orbitals of the metal carbonyl fragment. The following three lower energy orbitals of $\{HGeCr(CO)_4\}_2$ have b_{3g}, a_g and a_u symmetries, and they are all essentially composed of *d*-orbitals from the transition metal atoms. The inner b_{2u}, b_{2g} and b_{1u} symmetric orbitals of $\{HGeCr(CO)_4\}_2$ are M-E bonding in character, with the latter two describing π-type back-bonding interactions. The innermost orbitals of $\{HGeCr(CO)_4\}_2$ are of b_{3u} and a_g symmetries, and are essentially the bonding and anti-bonding combinations of lone pair orbitals of the two germanium centers with smaller contributions from unoccupied orbitals of the metal carbonyl fragment.

Taken as a whole, the diagram in Figure 3 shows that the metal-metal interactions in **1**–**6** arise from the combination of transition metal *d*-orbitals with both in-plane (σ-type) and out of plane (π-type) *p*-orbitals of the heavier main group atoms. Quantitatively, the biggest contribution to bonding comes from the b_{1g} symmetric HOMO as both of its constituent fragment orbitals are initially unoccupied. Although it is difficult to assign an E-M bond order for the complexes, the presence of four primarily E-M bonding orbitals with eight electrons is qualitatively consistent with four single bonds. The Wiberg E-M bond indices calculated for **1** and **4** are both somewhat less than one, however, at 0.69 and 0.56 respectively. There is no indication of a significant M-M or E-E bonding contribution as all orbitals that are bonding across the rhomboid M_2E_2 core are fully offset by their antibonding counterparts.

The mechanism of formation of **1**–**6** was also probed computationally. Given the evidence that, under photolysis in solution, the $M(CO)_5$ fragments react rapidly with σ-donors prior to further CO dissociation,[34] the formation of **1**–**6** is likely to involve pentacarbonyl intermediates. Therefore, we presume that, upon photoirradiation of the hexacarbonyls, loss of CO from the transition metal occurs, after which the $M(CO)_5$ fragment binds to the dimetallyne $(ER)_2$. This can take place via resonance form **II** or **III** (Scheme 1), leading to the formation of one or two donor-acceptor interactions, respectively.

Gas phase geometry optimizations conducted for the possible adducts of $(GeAr^{iPr4})_2$ with one or two $Cr(CO)_5$ fragments show that the complexes **II**-$Cr(CO)_5$ and $(CO)_5$Cr-**III**-$Cr(CO)_5$ (E = Ge) both represent stable minima on the potential energy hypersurface (Scheme 5). It is noteworthy that the complex with one coordinated $Cr(CO)_5$ fragment displays an elongated Ge-

Ge bond of 2.65 Å (compared to 2.2850(4)Å in $(GeAr^{iPr4})_2$),[1b] but the Ge-Ge distance in the complex with two donor-acceptor interactions is even longer at 2.97 Å. The significant lengthening of the Ge-Ge bond upon coordination of $(GeAr^{iPr4})_2$ to two $Cr(CO)_5$ fragments is consistent with the use of both main group element lone pairs for donor-acceptor bond formation. Consequently, the Ge-Ge bonding interaction in $(CO)_5Cr$-**III**-$Cr(CO)_5$ is exclusively due to the σ-type MO involving main group metal *p*-orbitals (HOMO−2 in Scheme 2), which also explains why the dissociation of $(CO)_5Cr$-**III**-Cr(CO) to two $(CO)_5CrGeAr^{iPr4}$ 'monomers' was calculated to be a thermoneutral process.

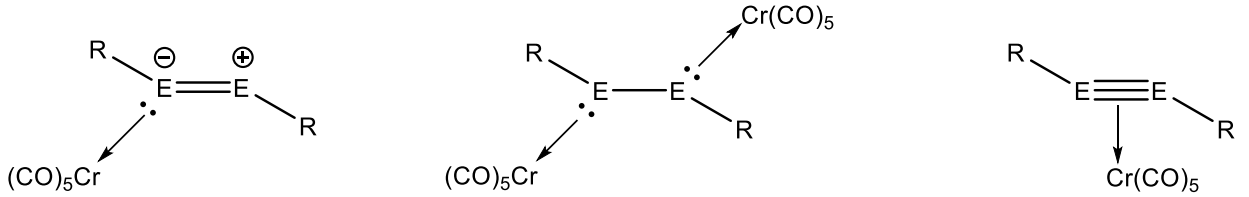

II-$Cr(CO)_5$ $(CO)_5Cr$-**III**-$Cr(CO)_5$ $(CO)_5Cr(\eta^2$-**I**)

Scheme 5: Schematic drawings of stable minima on the potential energy hypersurface of the reaction of $Cr(CO)_6$ with dimetallynes upon photoirradiation.

Further scans of the potential energy surface revealed a third possible intermediate in the formation of **1**–**6**, namely the complex $(CO)_5Cr(\eta^2$-**I**) (E = Ge), in which a single transition metal carbonyl binds to the Ge-Ge bond in η^2-fashion (Scheme 5). Somewhat surprisingly, the adduct $(CO)_5Cr(\eta^2$-**I**) is energetically slightly (18 kJ mol^{-1}) more stable than complex **II**-$Cr(CO)_5$. The Ge-Ge bond in $(CO)_5Cr(\eta^2$-**I**) is much shorter than in **II**-$Cr(CO)_5$, only 2.37 Å, owing to the coordination of the metal carbonyl fragment directly to the π-bond of $(GeAr^{iPr4})_2$ (HOMO in Scheme 2). Interestingly, the irradiation of $M(CO)_6$ (M = Cr, Mo, W) in the presence of excess bis(trimethylsilyl)ethyne (btmse) in *n*-hexane is known to lead to the formation of $(CO)_5M(\eta^2$-btmse),[35] which lends some credence to the argument that intermediates of the type $(CO)_5M(\eta^2$-**I**) might be involved in the formation of **1**–**6**.

At this point, the computational evidence for the mechanism of the formation of **1**–**6** remains inconclusive. The involvement of adducts of the type $(CO)_5M$-**III**-$M(CO)_5$ seems a less likely scenario as they are predicted to be prone to dissociation into $(CO)_5MEAr^{iPr4}$ that contain one unpaired electron at the heavier group 14 element E. Such radicals are expected to be highly

reactive species and therefore susceptible to various side reactions such as proton abstraction. For this reason, complexes of the type **II**-$M(CO)_5$ and $(CO)_5M(\eta^2$-**I**) seem more plausible candidates for reaction intermediates though it is difficult to envision the exact order of subsequent steps required for the formation of complexes **1**–**6** (interaction with another metal carbonyl, loss of CO and breakup of the EE bond). For this reason, we attempted to trap the postulated reaction intermediates **II**-$M(CO)_5$ or $(CO)_5M(\eta^2$-**I**) by reacting $(SnAr^{iPr4})_2$ with $Mo(CO)_5NMe_3$ at elevated temperatures. However, only unreacted starting materials or decomposition products could be identified with no indication of the formation of either **II**-$M(CO)_5$ or $(CO)_5M(\eta^2$-**I**). Further experimental and computational efforts to characterize the mechanism of the formation of **1**–**6** are ongoing.

CONCLUSION

We have prepared a series of novel metallo-germylyne and metallo-stannylyne complexes $\{Ar^{iPr4}EM(CO)_4\}_2$ (E = Ge, Sn; M = Cr, Mo, W) via insertion of neutral transition metal carbonyls into E-E triple bonds under UV irradiation. To the best of our knowledge, this represents a previously unreported transformation for the heavier group 14 alkyne analogues. The synthesized complexes were characterized by single crystal X-ray diffraction as well as IR and multinuclear NMR spectroscopies along with theoretical calculations at the density functional level of theory. All complexes feature a nearly planar rhomboid M_2E_2 core in which the E-M metal-metal bonding involves a combination of transition metal *d*-orbitals with both in-plane (σ-type) and out of plane (π-type) *p*-orbitals of the heavier main group atoms. Even though the conducted bonding analyses readily rationalize the singlet ground states and structures of $\{Ar^{iPr4}EM(CO)_4\}_2$, the exact mechanism of their formation remains unclear. Computational evidence suggests that the initial step in the mechanism involves a reaction between the photoactivated $M(CO)_5$ fragment with $(EAr^{iPr4})_2$, but neither one of the two predicted adducts could be isolated experimentally.

EXPERIMENTAL SECTION

General Considerations. All manipulations were carried out under strictly anaerobic and anhydrous conditions using modified Schlenk techniques or in a Vacuum Atmospheres HE-43

drybox. All solvents were trap-to-trap vacuum distilled and dried over 4 Å molecular sieves prior to use. The dimetallynes $(GeAr^{iPr_4})_2$ and $(SnAr^{iPr_4})_2$ were prepared according to literature procedures.[1b,c] Their purity was established spectroscopically. ^1H, $^{13}C\{^1H\}$ and $^{119}Sn\{^1H\}$ NMR spectra were recorded on Varian 400 and 600 MHz spectrometers and referenced internally to solvent signals or externally to Sn^nBu_4 in $CDCl_3$. The group 6 hexacarbonyls were purchased commercially and used as received. Infrared spectra were recorded as Nujol mulls between CsI plates on a Bruker Tensor 27 FTIR spectrometer. UV-visible spectra were recorded as dilute hexane solutions in 3.5 mL quartz cuvettes using an Olis 17 Modernized Cary 14 UV/Vis/NIR spectrophotometer. Melting points were determined on a Meltemp II apparatus using glass capillaries sealed with vacuum grease and are uncorrected.

Syntheses. Dimetallyne $(EAr^{iPr_4})_2$ (0.24 mmol; 0.235 and 0.258 g for Ge and Sn, respectively) and metal carbonyl $M(CO)_6$ (0.5 mmol; 0.110, 0.132 and 0.175 g for Cr, Mo and W, respectively) were dissolved in dry degassed hexane or pentane (20 mL) in a quartz Schlenk tube. The solution was irradiated for 24 hrs with a Rayonet-200 photo reactor with a wavelength range of 253–570 nm at approximately 35 W. A color change from dark green (Sn)/bright orange (Ge) to dark red (Sn)/dark brown (Ge) was observed. The solution was decanted and concentrated under reduced pressure to 5 mL then stored at –18°C to afford crystals of **1–3**, **5** and **6** that were suitable for X-ray crystallography. Crystals of **4** suitable for X-ray diffraction were grown from a saturated toluene solution.

$\{Ar^{iPr4}GeCr(CO)_4\}_2$ (1). Red crystals. Yield: 20 % (0.061 g). M.p. 235°C. ^1H NMR (600 MHz, C_6D_6, 298 K): 1.03 (d, *o*-CH(C*H*$_3$)$_2$, J_{HH} = 6 Hz, 24H), 1.47 (d, *o*-CH(C*H*$_3$)$_2$, J_{HH} = 6 Hz, 24 H), 3.60 (sept, *o*-C*H*(CH$_3$)$_2$, J_{HH} = 6 Hz, 8H), 7.01–7.05 (m, Ar, 12H), 7.20 (m, Ar, J_{HH} = 6 Hz, 2H), 7.32 (m, Ar, 8H). $^{13}C\{^1H\}$ NMR (C_6D_6, 150.6 MHz, 298 K): 24.1, 27.6, 31.6, 124.8, 128.9, 130.2, 133.4, 136.6, 142.8, 148.0, 162.6, 209.5 (CO), 232.6 (CO). λ_{max} (ε): 344 nm (3,760 L mol^{-1} cm^{-1}). IR (υ, cm^{-1}): 2018 (m), 1975 (m), 1939 (s).

$\{Ar^{iPr4}GeMo(CO)_4\}_2$ (2). Turquoise crystals, hexane solvate. Yield: 24 % (0.078 g)M.p. 265°C (dec). ^1H NMR (400 MHz, C_6D_6, 298 K): 1.06 (d, *o*-CH(C*H*$_3$)$_2$, J_{HH} = 6 Hz, 24H), 1.46 (d, *o*-CH(C*H*$_3$)$_2$, J_{HH} = 6 Hz, 24 H), 3.63 (sept, *o*-C*H*(CH$_3$)$_2$, J_{HH} = 6 Hz, 8H), 6.97 (t, Ar, J_{HH} = 6Hz, 4H), 7.01 (d, Ar, J_{HH} = 6Hz, 8H) 7.24 (t, Ar, J_{HH} = 6 Hz, 2H), 7.32 (d, Ar, J_{HH} = 6Hz, 4H). $^{13}C\{^1H\}$ NMR (C_6D_6, 150.6 MHz, 298 K): 24.4, 27.5, 31.5, 124.7, 128.9, 130.3, 133.3, 136.5,

142.5, 147.9, 162.6, 200.1 (CO), 221.9 (CO). λ_{max} (ε): 306 nm (3,300 L mol^{-1} cm^{-1}), 359 nm (4,500 L mol^{-1} cm^{-1}). IR (υ, cm^{-1}): 2017 (m), 1982 (s), 1946 (s).

{Ar^{iPr4}GeW(CO)$_4$}$_2$ (3). Turquoise crystals, hexane solvate. Yield: 25 % (0.092 g). M.p. 328–331°C. ^{1}H NMR (400 MHz, C_6D_6, 298 K): 1.06 (d, *o*-CH(C*H*$_3$)$_2$, 24H, J_{HH} = 6.8 Hz), 1.46 (d, *o*-CH(C*H*$_3$)$_2$, 24H), J_{HH} = 6.8 Hz), 3.60 (sept, *o*-C*H*(CH$_3$)$_2$, J_{HH} = 6.8 Hz, 8H), 7.00–7.04 (m, Ar, 12H), 7.27 (m, Ar, 3H), 7.35 (d, Ar, J_{HH} = 6.8 Hz, 3H). ^{13}C{^{1}H} NMR (C_6D_6, 150.6 MHz, 298 K): 23.8, 26.9, 124.2, 128.5, 129.8, 133.1, 135.9, 142.4, 142.6, 147.2, 163.1, 190.0 (CO), 207.4 (CO). λ_{max} (ε): 301 nm (80,000 L mol^{-1} cm^{-1}), 357 nm (82,000 L mol^{-1} cm^{-1}), 597 nm (610 L mol^{-1} cm^{-1}). IR (υ, cm^{-1}): 2012 (s), 1977 (s), 1940 (s).

{Ar^{iPr4}SnCr(CO)$_4$}$_2$ · 2C$_7$H$_8$ (4 · 2C$_7$H$_8$). Red crystals, toluene solvate. Yield 20 % (0.065 g) M.p. 245°C (dec.). ^{1}H NMR (400 MHz, C_6D_6, 298 K): 1.03 (d, *o*-CH(C*H*$_3$)$_2$, 24H, J_{HH} = 6.8 Hz), 1.52 (d, *o*-CH(C*H*$_3$)$_2$, 24H, J_{HH} = 6.8 Hz), 3.59 (sept, *o*-C*H*(CH$_3$)$_2$, 8H, J_{HH} = 6.8 Hz), 6.98–7.07 (m, Ar, 14H), 7.29 (t, Ar, 2H), 7.43 (d, Ar, 4H). ^{13}C{^{1}H} NMR (C_6D_6, 150.6 MHz, 298 K): 2.5. 6.9, 11.8, 122.7, 128.7, 130.6, 133.3, 137.4, 147.9, 151.4, 226.0 (CO), 254.3 (CO). ^{119}Sn{^{1}H} NMR (223.6 MHz, C_6D_6, 298 K): 2177.7. λ_{max} (ε): 370 nm (17,500 L mol^{-1} cm^{-1}), 449 nm (4,200 L mol^{-1} cm^{-1}). IR (υ, cm^{-1}): 1982 (s), 1945 (s), 1934 (s), 1914 (s).

{Ar^{iPr4}SnMo(CO)$_4$}$_2$ (5). Brown red crystals. Yield 18 % (0.063 g). M.p. > 300°C. ^{1}H NMR (600 MHz, C_6D_6, 298 K): 1.04 (d, *o*-CH(C*H*$_3$)$_2$, J_{HH} = 6 Hz, 24H), 1.52 (d, *o*-CH(C*H*$_3$)$_2$, J_{HH} = 6 Hz, 24H), 3.56 (sept, *o*-C*H*(CH$_3$)$_2$, J_{HH} = 6 Hz, 8H), 6.96 (t, J_{HH} = 7.2 Hz, Ar, 4H), 7.04 (d, Ar, J_{HH} = 6.8 Hz, 8H), 7.33 (t, Ar, J_{HH} = 7.2 Hz, 2H), 7.45 (d, Ar, J_{HH} = 7.6 Hz, 4H). ^{13}C{^{1}H} NMR (C_6D_6, 150.6 MHz, 298 K): 23.5, 27.0, 31.04, 124.2, 128.3, 130.3, 131.9, 135.5, 144.8, 147.5, 201.1 (CO), 223.4 (CO). ^{119}Sn{^{1}H} NMR (223.6 MHz, C_6D_6, 298 K): 2250.9. λ_{max} (ε): 318 nm (1,100 L mol^{-1} cm^{-1}), 374 nm (1,850 L mol^{-1} cm^{-1}). IR (υ, cm^{-1}): 2005 (s), 1955 (s), 1940 (s), 1917 (s).

{Ar^{iPr4}SnW(CO)$_4$}$_2$ (6). Brown red crystals. Yield 12 % (0.023 g). M.p. > 300°C. ^{1}H NMR (600 MHz, C_6D_6, 298 K): 1.03 (d, *o*-CH(C*H*$_3$)$_2$, J_{HH} = 6 Hz, 24H), 1.52 (d, *o*-CH(C*H*$_3$)$_2$, J_{HH} = 6 Hz, 24H), 3.55 (sept, *o*-C*H*(CH$_3$)$_2$, J_{HH} = 6 Hz, 8H), 7.00 (t, Ar, 4H), 7.05 (d, Ar, J_{HH} = 6 Hz, 8H), 7.36 (t, Ar, J_{HH} = 6 Hz, 2H), 7.47 (d, Ar, J_{HH} = 6 Hz, 4H). ^{13}C{^{1}H} NMR (C_6D_6, 150.6 MHz, 298 K): 24.1, 27.6, 31.6, 124.7, 125.1, 129.1, 132.7, 133.1, 136.2, 145.9, 148.0, 191.3 (CO), 210.0 (CO). ^{119}Sn{^{1}H} NMR (223.6 MHz, C_6D_6, 298 K): 2134.0. λ_{max} (ε): 312 nm (13,000 L mol^{-1} cm^{-1}), 365 nm (9,500 L mol^{-1} cm^{-1}). IR (υ, cm^{-1}): 1999 (s), 1953 (s), 1934 (s), 1910 (s).

X-Ray Crystallography. Crystals of **1**–**6** suitable for single crystal X-ray diffraction studies were covered in silicone oil and attached to a glass fiber on the mounting pin at the goniometer. Crystallographic measurements were collected at 90 K with a Bruker APEX II DUO or Bruker Apex II CCD diffractometer using Mo K_α (λ = 0.71073 Å) or Cu (λ = 1.54178 Å) radiation. The crystal structures were corrected for Lorentz and polarization effects with SAINT[36] and absorption using Blessing's method as incorporated into the program SADABS.[37] The SHELXTL program was used to determine the space groups and set up the initial files.[38] The structures were determined by direct methods using the program SHELXS and refined with the program SHELXL.[39] All non-hydrogen atoms were refined with anisotropic displacement parameters. Hydrogen atoms were placed in idealized positions throughout the refinement process and refined as riding atoms with individual isotropic refinement parameters. For compounds **2** and **3**, SQUEEZE was used to remove disordered hexane. A summary of data collection and refinement parameters is given in the ESI.

Computational Details. Optimized geometries and vibrational frequencies were calculated with the Gaussian09 program[40] using density functional theory and the PBE0 hybrid functional.[41] Alrichs' triple-ζ quality basis sets (def-TZVP) were used for all atoms except tin for which a corresponding pseudopotential basis set was employed.[42] Dispersion interactions were modeled by applying Grimme's empirical dispersion correction with Becke−Johnson damping (D3BJ).[43] Frequency calculations were performed on all located stationary points in order to verify that they represented true minima on the potential energy surface. Wiberg bond indices were calculated in the NAO basis using the NBO code as implemented in Gaussian09.[44] Optimized coordinates for calculated structures are given in the ESI.

References

1. (a) Pu, L.; Twamley, B.; Power, P. P. *J. Am. Chem. Soc.* **2000**, *122*, 3524-3525. (b) Stender, M.; Phillips, A. D.; Wright, R. J.; Power, P. P. *Angew. Chem. Int. Ed.* **2002**, *41*, 1785-1787. (c) Phillips, A. D.; Wright, R. J.; Olmstead, M. M.; Power, P. P. *J. Am. Chem. Soc.* **2002**, *124*, 5930-5931. (d) Sekiguchi, A.; Kinjo, R.; Ichinohe, M. *Science* **2004**, *305*, 1755-1757. (e) Wiberg, N.; Vasisht, S. K.; Fischer, G.; Mayer, P. *Z. Anorg. Allg. Chem.* **2004**, *630*, 1823-1828. (f) Spikes, G. H.; Giuliani, J. R.; Augustine, M. P.;

Nowik, I.; Herber, R. H.; Power, P. P. *Inorg. Chem.* **2006**, *45*, 9132-9136. (g) Sugiyama, Y.; Sasamori, T.; Hosoi, Y.; Furukawa, Y.; Takagi, N.; Nagase, S.; Tokitoh, N. *J. Am. Chem. Soc.* **2006**, *128*, 1023-1031. (h) Sasamori, T.; Han, J. S.; Hironaka, K.; Takagi, N.; Nagase, S.; Tokitoh, N. *Pure Appl. Chem.* **2010**, *82*, 603-612.

2. (a) Power, P. P. *Chem. Commun.* **2003**, 2091-2101. (b) Rivard, E.; Power, P. P. *Inorg Chem.* **2007**, *46*, 10047-10064. (c) Power, P. P. *Organometallics* **2007**, *26*, 4362-4372. (d) Fischer, R. A.; Power, P. P. *Chem. Rev.* **2010**, *110*, 3877-3923. (e) Lee, V. Y.; Sekiguchi, A. *Organometallic Compounds of Low-Coordinate Si, Ge, Sn and Pb: From Phantom Species to Stable Compounds*, John Wiley & Sons, Ltd, Chichester, UK, 2010.
3. (a) Olmstead, M. M.; Simons, R. S.; Power, P. P. *J. Am. Chem. Soc.* **1997**, *119*, 11705-11706. (b) Pu. L.; Senge, M. O.; Olmstead, M. M.; Power, P. P. *J. Am. Chem. Soc*. **1998**, *120*, 12682-12683. (c) Sekiguchi, A.; Kinjo, R.; Ichinohe, M. *Synt. Met.* **2009**, *159*, 773-775. (d) Kinjo, R.; Ichinohe, M.; Sekiguchi, A. *J. Am. Chem. Soc.* **2007**, *129*, 26-27.
4. (a) Cui, C.; Olmstead, M. M.; Fettinger, J. C.; Spikes G. H.; Power, P. P. *J. Am. Chem. Soc.* **2005**, *49*, 17530-17541. (b) Yamaguchi, T.; Sekiguchi, A.; Driess, M. *J. Am. Chem. Soc.* **2010**, *132*, 14061-14063.
5. (a) Spikes, G. H.; Fettinger, J. C.; Power, P. P. *J. Am. Chem. Soc.* **2005**, *127*, 12232-12233. (b) Rivard, E.; Steiner, J.; Fettinger, J. C.; Giuliani, J. R.; Augustine, M. P.; Power, P. P. *Chem. Commun.* **2007**, 4919-4921. (c) Peng, Y.; Brynda, M.; Ellis, B. D.; Fettinger, J. C.; Rivard, E.; Power, P. P. *Chem. Commun.* **2008**, 6042-6044.
6. (a) Li, J.; Schenk, C.; Goedecke, C.; Frenking, G.; Jones, C. *J. Am. Chem. Soc.* **2011**, *133*, 18622-18625. (b) Hadlington, T. J.; Hermann, M.; Li, J.; Frenking, G.; Jones, C. *Angew. Chem. Int. Ed.* **2013**, *52*, 10199-10203. (c) Hadlington, T. J.; Jones, C. *Chem. Commun.* **2014**, 50, 2320-2321.
7. (a) Takeuchi, K.; Ikoshi, M.; Ichinohe, M.; Sekiguchi, A. *J. Organomet. Chem.* **2011**, *696*, 1156-1162. (b) Takeuchi, K.; Ichinohe, M.; Sekiguchi, A. *Organometallics* **2011**, *30*, 2044-2050. (c) Takeuchi, K.; Ikoshi, M.; Ichinohe, M.; Sekiguchi, A. *J. Am. Chem. Soc.* **2010**, *132*, 930-931.
8. (a) Kinjo, R.; Ichinohe, M.; Sekiguchi, A.; Takagi, N.; Sumimoto, M. Nagase, S. *J. Am. Chem. Soc.* **2007**, *129*, 7766-7767. (b) Peng, Y.; Ellis, B.; Wang, X.; Fettinger, J.; Power, P. *Science* **2009**, *325*, 1668-1670. (c) Cui, C.; Olmstead, M. M.; Power, P. P. *J. Am.*

Chem. Soc. **2004**, *126*, 5062-5063. (d) Han, J. S.; Sasamori, T.; Mizuhata, Y.; Tokitoh, N. *Dalton Trans.* **2010**, *39*, 9238-9240. (e) Han, J. S.; Sasamori, T.; Mizuhata, Y.; Tokitoh, N. *J. Am. Chem. Soc.* **2010**, *132*, 2546-2547. (f) Sasamori, T.; Sugahara, T.; Agou, T.; Guo, J.-D.; Nagase, S.; Streubel, R.; Tokitoh, N. *Organometallics* **2015**, *34*, 2106-2109. (g) Sasamori, T.; Sugahara, T.; Agou, T.; Sugamata, K.; Guo, J.-D.; Nagase, S.; Tokitoh, N. *Chem. Sci.* **2015**, *6*, 5526-5530. (h) Hadlington, T. J.; Li, J.; Hermann, M.; Davey, A.; Frenking, G.; Jones, C. *Organometallics* **2015**, *34*, 3175-3185.

9. Wang, X.; Peng, Y.; Olmstead M. M.; Hope, H.; Power, P. P.; *J. Am. Chem. Soc.* **2010**, *132*, 13150-13151.
10. Ishida, S.; Sugawara, R.; Misawa, Y; Iwamoto, T. *Angew. Chem. Int. Ed.* **2013**, *52*, 12869-12873.
11. Yamaguchi, T.; Ichinohe, M.; Sekiguchi, A.; *New J. Chem.* **2010**, *34*, 1544-1546.
12. (a) Weidenbruch, M.; Stilter, A.; Schlaefke, J.; Peters, K.; von Schnering, H. G. *J. Organomet. Chem.* **1995**, *501*, 67-70. (b) Weidenbruch, M.; Stilter, A.; Peters, K.; von Schnering, H. G. *Z. Anorg. Allg. Chem.* **1996**, *622*, 534-538. (c) Schneider, J.; Czap, N.; Bläser, D.; Boese, R.; Ensling, J.; Gütlich, P.; Janiak, C. *Chem. Eur. J.* **2000**, *6*, 468-474. (d) Bareš, J.; Richard, P.; Meunier, P.; Pirio, N.; Padělková, Z.; Černošek, Z.; Císařová, I.; Růžička, A. *Organometallics* **2009**, *28*, 3105-3108. (e) Weidenbruch, M.; Stilter, A.; Saak, W.; Peters, K.; von Schnering, H. G. *J. Organomet. Chem.* **1998**, *560*, 125-129. (f) Schneider, J.; Czap, N.; Blaser, D.; Boese, R. *J. Am. Chem. Soc.* **1999**, *121*, 1409-1410.
13. Eichler, B. E.; Phillips, A. D.; Haubrich, S. T.; Mork, B. V.; Power, P. P. *Organometallics* **2002**, *21*, 5622-5627.
14. Filippou, A. C.; Portius, P.; Philippopoulos, A. I.; Rohde, H. *Angew. Chem. Int. Ed.* **2003**, *42*, 445-447.
15. Kayran, C.; Kozanoglu, F.; Özkar, S.; Saldamli, S.; Tekkaya, A.; Kreiter, C. G. *Inorg. Chim. Acta* **1999**, *284*, 229-236.
16. Kraihanzel, C. S.; Cotton, F. A. *Inorg. Chem.* **1961**, *2*, 533-540.
17. Magee, T. A.; Matthews, C. N.; Wang, T. S.; Wotiz, J. H. *J. Am. Chem. Soc.* **1961**, *83*, 3200-3203.

18. (a) Summerscales, O. T.; Wang, X.; Power, P. P. *Angew. Chem. Int. Ed.* **2010**, *49*, 4788-4790. (b) Summerscales. O, T.; Jimenez-Halla, O. C.; Merino, G.; Power, P. P. *J. Am. Chem. Soc.* **2011**, *133*, 180-183.
19. Takeuchi, K.; Ichinohe, M.; Sekiguchi, A.; Guo, J-D.; Nagase, S. *Organometallics* **2009**, *28*, 2658-2660.
20. Spikes, G. H.; Peng, Y.; Fettinger, J. C.; Steiner, J.; Power, P. P. *Chem. Commun.* **2005**, 6041-6043.
21. Pyykkö, P.; Atsumi, M. *Chem. Eur. J.* **2009**, *15*, 186-197.
22. Lappert, M. F.; Miles, S. J.; Power, P. P.; Carty, A. J.; Taylor, N. J. *Chem. Commun.* **1977**, 458-459.
23. Jutzi, P.; Steiner, W.; Konig, E.; Huttner, G.; Frank, A.; Schubert, U. *Chem. Ber.* **1978**, *111*, 606-614.
24. (a) Desclaux, J. P. *At. Data Nucl. Data Tables* **1973**, *12*, 311-406. (b) Kutzelnigg, W. *Angew. Chem. Int. Ed. Engl.* **1984**, *23*, 272-295. (c) Mann, J. B. *Atomic Structure Calculations II. Hartree-Fock Wave Functions and Radial Expectation Values: Hydrogen to Lawrencium*, LA-3691, Los Alamos Scientific Laboratory, Los Alamos, New Mexico, USA, 1968.
25. Pu, L.; Twamley, B.; Haubrich, S. T.; Olmstead, M. M.; Mork, B. V.; Simons, R. S.; Power, P. P. *J. Am. Chem. Soc.* **2000**, *122*, 650-656.
26. Kuhl, O.; Lonnecke, P.; Heinicke, J. *Inorg. Chem.* **2003**, *42*, 2836-2838.
27. Hicks, J.; Hadlington, T. J.; Schenk, C.; Li, J.; Jones, C. *Organometallics* **2013**, *32*, 323-329.
28. Wang, B.; Zhu, B.; Xu, S.; Zhou, X. *Organometallics* **2003**, *22*, 4842-4852.
29. du Mont, W.-W.; Lange, L.; Pohl, S.; Saak, W. *Organometallics* **1990**, *9*, 1395-1399.
30. Al-Rafia, S. M. I.; Momeni, M. R.; Ferguson, M. J.; McDonald, R.; Brown, A.; Rivard, E. *Organometallics* **2013**, *32*, 6658-6665.
31. Cotton, J. D.; Davison, P. J.; Goldberg, D. E.; Lappert, M. F.; Thomas, K. M. *J. Chem. Soc. Chem. Comm.* **1974**, 893-895.
32. Lin, J. T.; Shan, C. H.; Fang, D.; Liu, L-K.; Hsiou, Y.; *J. Chem. Soc. Dalton Trans.* **1988,** 1397-1399.

33. Kircher, P.; Huttner, G.; Heinze, K.; Schiemenz, B.; Zsolnai, L.; Büchner, M.; Driess, A. *Eur. J. Inorg. Chem.* **1998**, 703-720.
34. (a) Abel, E. W.; Stone, F. G. A. *Q. Rev. Chem. Soc.* **1970**, *24*, 498-552. (b) Welch, J. A.; Peters, K. S.; Vaida, V. *J. Phys. Chem.* **1982**, *86*, 1941-1947.
35. Grevels, F. W.; Jacke, J.; Goddard. R.; Lehmann, C. W.; Özkar, S.; Saldamli, S. *Organometallics* **2005**, *24*, 4613-4623.
36. Bruker *SMART APEX* (2013.6-2) *and SAINT* (Version 7.68s), Bruker AXS Inc., Madison, Wisconsin, USA, 2009 and 2013.
37. (a) Sheldrick, G. M. *SADABS 'Siemens Area Detector Absorption Correction'*, Universität Göttingen, Göttingen, Germany, 2012. (b) Blessing, R. H. *Acta Cryst. A* **1995**, *51*, 33-38.
38. Sheldrick, G. M. *SHELXTL* (Version 6.1), Bruker AXS Inc., Madison, Wisconsin, USA, 2000.
39. Sheldrick, G. M. *Acta Cryst. A.* **2008**, *64*, 112-122.
40. Gaussian 09, Revision D.01, M. J. Frisch, G. W. Trucks, H. B. Schlegel, G. E. Scuseria, M. A. Robb, J. R. Cheeseman, G. Scalmani, V. Barone, B. Mennucci, G. A. Petersson, H. Nakatsuji, M. Caricato, X. Li, H. P. Hratchian, A. F. Izmaylov, J. Bloino, G. Zheng, J. L. Sonnenberg, M. Hada, M. Ehara, K. Toyota, R. Fukuda, J. Hasegawa, M. Ishida, T. Nakajima, Y. Honda, O. Kitao, H. Nakai, T. Vreven, J. A. Jr. Montgomery, J. E. Peralta, F. Ogliaro, M. Bearpark, J. J. Heyd, E. Brothers, K. N. Kudin, V. N. Staroverov, R. Kobayashi, J. Normand, K. Raghavachari, A. Rendell, J. C. Burant, S. S. Iyengar, J. Tomasi, M. Cossi, N. Rega, M. J. Millam, M. Klene, J. E. Knox, J. B. Cross, V. Bakken, C. Adamo, J. Jaramillo, R. Gomperts, R. E. Stratmann, O. Yazyev, A. J. Austin, R. Cammi, C. Pomelli, J. W. Ochterski, R. L. Martin, K. Morokuma, V. G. Zakrzewski, G. A. Voth, P. Salvador, J. J. Dannenberg, S. Dapprich, A. D. Daniels, Ö. Farkas, J. B. Foresman, J. V. Ortiz, J. Cioslowski, D. J. Fox, Gaussian, Inc.: Wallingford, Connecticut, USA, 2009.
41. (a) Perdew, J. P.; Burke, K.; Ernzerhof, M. *Phys. Rev. Lett.*, **1996**, *77*, 3865-3868. (b) Perdew, J. P.; Ernzerhof, M.; Burke, K. J. *Chem. Phys.*, **1996**, *105*, 9982-9985. (c) Perdew, J. P.; Burke, K.; Ernzerhof, M. *Phys. Rev. Lett.*, **1997**, *78*, 1396. (d) Adamo, C.; Barone, V. *J. Chem. Phys.*, **1999**, *110*, 6158-6170.

42. (a) Schaefer, A.; Huber, C.; Ahlrichs, R. *J. Chem. Phys.*, **1994**, *100*, 5829-5835. (b) Andrae, D.; Haeussermann, U.; Dolg, M.; Stoll, H.; Preuss, H. *Theor. Chim. Acta* **1990**, *77*, 123-141.
43. (a) Grimme, S.; Ehrlich, S.; Goerigk, L. *J. Comput. Chem.*, **2011**, *32*, 1456−1465. (b) Grimme, S.; Antony, J.; Ehrlich, S.; Krieg, H. *J. Chem. Phys.* **2010**, *132*, 154104−154119.
44. Wiberg, K. B. *Tetrahedron* **1968**, *24*, 1083−1096.